arXiv:1610.09579v1 [math.DS] 29 Oct 2016

Billiards in near rectangles

Yilong Yang, Haibin Chang

November 1, 2016

1 Introduction

Inside a polygonal billiard table, a billiard ball travels in straight line until it hits an edge. The billiard ball bounces off an edge obeying the law of reflection, i.e. the angle of incidence equals the angle of reflection. See Figure 1.

The trajectory of the billiard ball is called a *billiard path*. The path is *periodic* if the ball repeats the same path over and over again. We ignore cases where the billiard ball hits one of the vertices of the billiard table.

One major question in this subject is the following: Does every polygon admit a periodic billiard path? It is known that all polygons whose angles are rational multiple of π have a periodic billiard path, see [1] and [3]. Schwartz has shown that all triangles with all angles smaller than 100 degree have periodic billiard path [4], [5]. In another paper by Hooper and Schwartz, it is shown that all triangles near enough to isosceles triangles have periodic billiard paths [2].

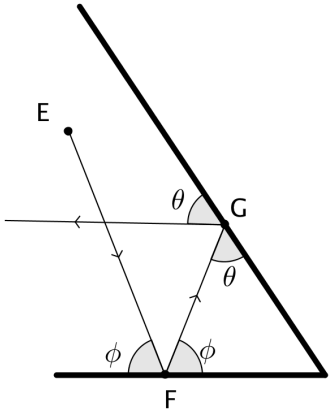

Figure 1: Law of Reflection

In this paper, we consider quadrilaterals which are close to being rectangles. The space $\mathcal{Q}$ of quadrilaterals (modulo similarity) can be "considered" as a subset of the $\mathbb{R}^4$, see Section 2.2. The main result of this paper is the following:

Theorem 1. *For every rectangle $r \in \mathcal{Q}$, there exists an open neighborhood $U \subset \mathcal{Q}$ containing r, such that every quadrilateral in U has a periodic billiard path.*

Theorem 2.2.4 will provide an explicit neighborhood U for the special case when r is a square.

2 Preliminary

2.1 Tools for Studying Billiards

Consider a right triangle in Figure 2. Suppose the billiard ball starts from point D moving upwards, perpendicular to side BC. Then it will hit the point E, reflect to hit point F, and then reflect to hit point G. We will leave it to the reader to show that $\angle x = \frac{\pi}{2}$.

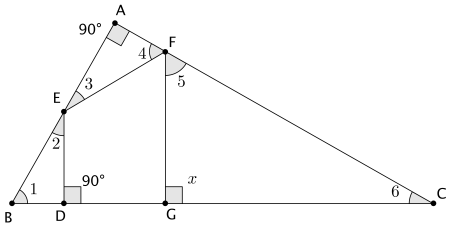

Figure 2: Right Triangle

The implication is that: after the ball hit G, it would bounce back along the exact same trajectory, and continues periodically. So, all right triangles have this periodic billiard path.

If we label the sides CB, BA, AC using $0, 1, 2$ respectively, then the sequence 012021 represents the order in which the trajectory hits the sides of the polygon. We call this finite sequence the *orbit type* of the periodic path, and the length of the orbit type (in the example above, 6) the *combinatorial length*.

A very useful tool to study billiard paths is the unfolding. See [6] also.

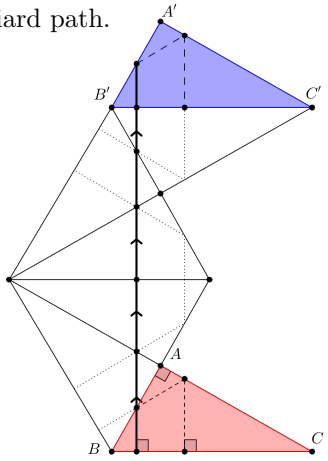

Figure 3: Unfolding for right triangle

Definition 2.1.1. *Given any orbit type $W = w_1w_2w_3 \dots w_n$, and any polygon P, the corresponding **unfolding** is a sequence of polygons $U(W, P) = P_0P_1P_2 \dots P_n$, such that $P_0 = P$, and each P_j is obtained by reflecting P_{j-1} along the edge w_j for $j \geq 1$.*

For example, in Figure 3, each time the ball hits an edge of the polygon, instead of reflecting the billiard path, we reflect the polygon and keep the path straight. The straight line in the unfolding will "correspond" to the original periodic path. Note that the two shaded triangles in Figure 3 are related by a translation along the direction of the billiard trajectory. Also, this translation requires a number of 6 reflection, which is exactly the combinatorial length of the orbit.

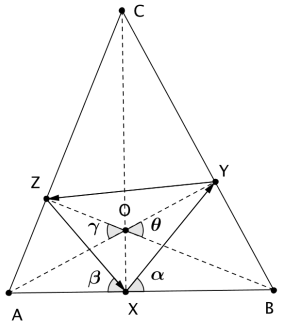

Figure 4: Fagnano Path

Next, let us look at the famous Fagnano orbit. For any acute triangle, we can connect the three feet of the altitudes, as in Figure 4. Then the orbit XY, YZ, ZX is actually a periodic billiard path. The proof is as follows:

Clearly points X, Y, B, O lies on a circle, and A, X, O, Z on another circle. So $\alpha = \theta = \gamma = \beta$. Hence, the path obey the law of reflection at the point X, and similarly at Y, Z.

By labelling AB, BC, CA using $0, 1, 2$ respectively, we can "represent" this periodic path by the word 012 (which has length 3). However, after 3 reflections in the unfolding(see Figure 5), the resultant polygon $(A'B'C')$ is not a translation of the original polygon (ABC).

The reason is that each reflection of the polygon changes its orientation. In order to have a translation, we need an even number of reflections. So if a periodic path can be "represented" by a word P of odd length (in the example above, 012), then we define its orbit type to be $P^2(012012)$, so that the first polygon (ABC) and last polygon $(A''B''C'')$ in the unfolding are related by a translation.

Of course, we can always reflect a polygon according to some arbitrary word. Then one important question is, given a word W, can we always find a corresponding periodic billiard path in some given polygon P? We have the following Lemma:

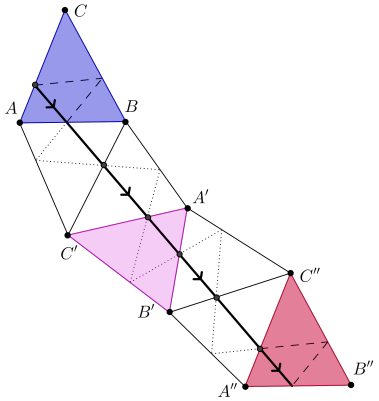

Figure 5: Unfolding for Fagnano path

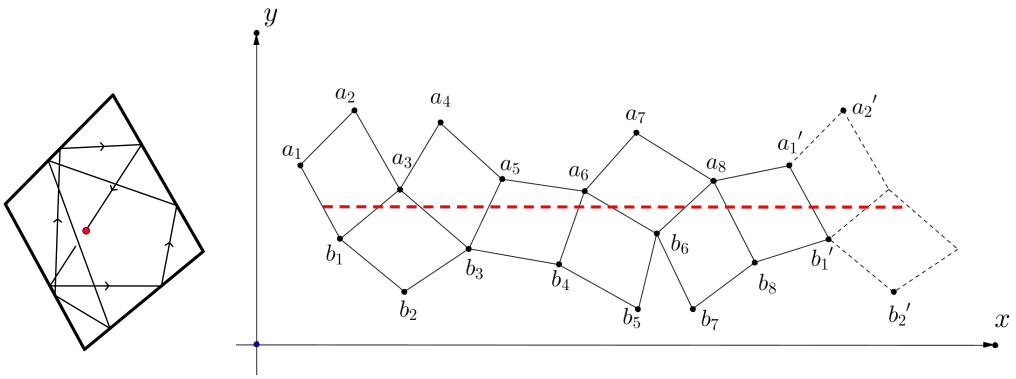

(a) (b)

Figure 6

Lemma 2.1.2. *For an even word W and a polygon P, there exists a periodic billiard path on P with the orbit type W if and only if:*

1. *The first and the last polygon in the unfolding $U(W, P)$ are related by a translation. AND*
2. *There exists a straight line segment, parallel to the direction of the translation, that stays within the unfolding and does not touch any of the vertex.*

To illustrate the second condition, let's look at Figure 6b, which is the unfolding for the periodic billiard path in Figure 6a. Assuming Condition 1 is satisfied, then a polygon has this periodic billiard path if and only if we can "fit" the red dashed line into the corresponding unfolding. (i.e. in Figure 6b, if we choose the direction of the translation as our x-axis, then we need the y-coordinate of a_i to be larger than that of b_j for any i and j.)

2.2 The space of quadrilaterals

Consider the space of all quadrilaterals (up to similarity), call it $\mathcal{Q}$. For any quadrilateral, we can split it into two triangles by drawing a diagonal. Each triangle is uniquely determined by two of its angles. So, any quadrilateral is determined by four parameters, a, b, c, d, as shown in Figure 7. The parameters of the square are $(\frac{\pi}{4}, \frac{\pi}{4}, \frac{\pi}{4}, \frac{\pi}{4})$, and rectangles are on the line

$$\{(a, b, c, d) : a = c, b = d, a + b = \tfrac{\pi}{2}\}.$$

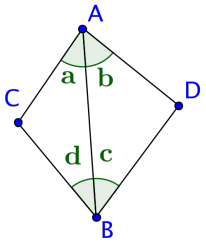

Figure 7: Four Parameters

For each orbit type W, we call the set of all quadrilaterals with this orbit type the *orbit tile* $O(W)$ of the orbit type.

Definition 2.2.1. *A orbit type W is called **stable** if the orbit tile $O(W)$ is a nonempty open set. Otherwise, W is unstable.*

We will use the following criterion for the stability of an orbit type. See [6]

Lemma 2.2.2. *For $O(W) \neq \emptyset$, an orbit type W is* stable *if and only if the number of times each sides of the polygon appears in an odd position in the orbit type equals the number of times it appears in an even position.*

For example, the orbit type 012021 is not stable, because 1 appears twice in even positions (and does not appear at odd position). Also, 012012 is stable.

Now we shall restate our main theorems more precisely.

Definition 2.2.3. *For $\varepsilon > 0$, a quadrilateral with parameter (a_1, a_2, a_3, a_4) is called ε-near square if $\left|a_i - \frac{\pi}{4}\right| < \varepsilon$ for any i.*

Theorem 2.2.4. *The set of all $\frac{\pi}{107}$-near square quadrilaterals is covered by finitely many orbit tiles.*

Theorem 2.2.5. *An open neighborhood of the rectangle line in the space $\mathcal{Q}$ can be covered by finitely many orbit tiles.*

3 Proof of Theorem 2.2.4

3.1 α-β plane

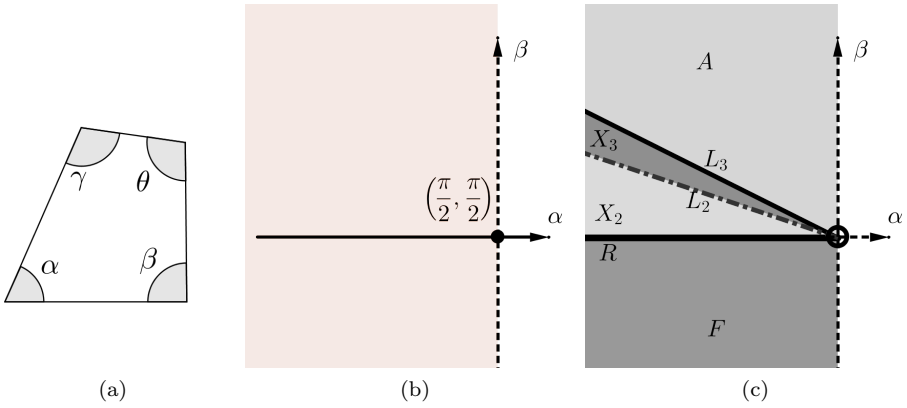

Figure 8

In this section, we will introduce a way of thinking about quadrilaterals. This will help us prove Theorem 2.2.4.

Let q be a quadrilateral. If q is not rectangle, then we can choose an acute angle α. For the two angles adjacent to α, we pick the smaller one (or either one, if they are equal), and call it β, as shown in Figure 8a. If q is a rectangle, then we let $\alpha = \frac{\pi}{2}, \beta = \frac{\pi}{2}$. Then, every quadrilateral will be characterized by some point on the α-β plane, which consists of the left half plane $\left(\alpha < \frac{\pi}{2}\right)$ and the origin $\left(\alpha = \frac{\pi}{2}, \beta = \frac{\pi}{2}\right)$, as shown in Figure 8b.

Note that a quadrilateral q being close to the $\left(\frac{\pi}{2}, \frac{\pi}{2}\right)$ point on the α-β plane does not tell anything about the "near-squareness" of the quadrilateral. For example, the point $\left(\frac{\pi}{2}, \frac{\pi}{2}\right)$ represents the set of all rectangles (including those rectangles that are not "near-square" at all).

To prove Theorem 2.2.4, we chop the left half plane into 8 regions. We show that an $\frac{\pi}{107}$-near square q has a periodic billiard path whose orbit type only depends on the region.

Region in α-β plane	in Figure 8c	orbit type	note
$\left(\frac{\pi}{2}, \frac{\pi}{2}\right)$	origin	0202	Rectangles
$\alpha < \frac{\pi}{2}, \beta < \frac{\pi}{2}$	F	012012	Section 3.2
$\alpha < \frac{\pi}{2}, \beta = \frac{\pi}{2}$	R	012021	Section 3.3
$\alpha < \frac{\pi}{2}, \alpha + 2\beta > \frac{3}{2}\pi$	A	01203213	Section 3.4
$\alpha < \frac{\pi}{2}, \alpha + 3\beta < 2\pi, \beta > \frac{\pi}{2}$	X_2	$0(13)^2013131310(31)^203$	Section 3.5
$\alpha < \frac{\pi}{2}, \alpha + 3\beta > 2\pi, \alpha + 2\beta < \frac{3}{2}\pi$	X_3	$0(13)^30(13)^2131(31)^20(31)^303$	Section 3.5
$\alpha < \frac{\pi}{2}, \alpha + 3\beta = 2\pi$	L_2	01313103	Section 3.6
$\alpha < \frac{\pi}{2}, \alpha + 2\beta = \frac{3}{2}\pi$	L_3	0131313103	Section 3.6

3.2 Adjacent acute angles

In this section, we will prove the following:

Proposition 3.2.1. *If q is $\frac{\varepsilon}{12}$-near square, and it has two adjacent acute angles, then q has a periodic billiard path.*

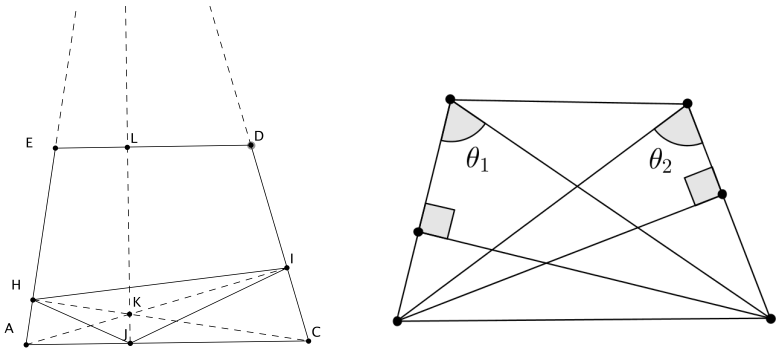

(a) (b)

Figure 9

We know that in every acute triangle, there's a periodic billiard path, the Fagnano orbit. The orbit type is 012012. Now suppose a near square have two adjacent acute angles. Then we can complete this near square to an acute triangle, and then find the Fagnano orbit, as shown in Figure 9a. Then since the quadrilateral is near square, two of the altitudes have to be really flat, so the Fagnano orbit stays inside this near square. This gives a periodic billiard path of the near square, and let us give this orbit a name, orbit F.

So, the central question now is how near square this path require. Let us consider Figure 9b. The critical condition is clearly that θ_1 and θ_2 as shown are smaller than $\frac{\pi}{2}$. We will need the following:

Lemma 3.2.2. *Let $ABCD$ be a quadrilateral as shown in Figure 10. Suppose $|\alpha_i - \frac{\pi}{4}| < \varepsilon$ for any i, and $\varepsilon < \frac{\pi}{12}$, then $|\beta_j - \frac{\pi}{4}| < 3 \cdot \varepsilon$ for any j.*

The proof of this lemma is trigonometric (using Sine Rule) and some estimates using Mathematica. We will leave the proof of this lemma to the reader.

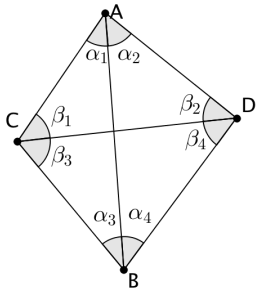

Figure 10

Proof of Prop 3.2.1. Suppose quadrilateral q is $\frac{\pi}{12}$ near square. Let θ_1 and θ_2 be the angle shown in figure 9b. By the above discussion, it suffice to show that $\theta_i < \frac{\pi}{2}, i = 1, 2$. Depending on the choice of diagonal used in the parameterization, one of the two angles θ_i satisfies $\left|\theta_i - \frac{\pi}{4}\right| < \frac{\pi}{2}$. By the lemma, the other angle satisfies $\left|\theta_j - \frac{\pi}{4}\right| < \frac{\pi}{4}$ □

3.3 Acute angle adjacent to a right angle

Proposition 3.3.1. *If q is $\frac{\pi}{12}$-near square, and it has a right angle adjacent to an acute angle, then q has a periodic billiard path.*

The proof is the same as the proof of proposition 3.2.1. In this case, we need to show the angle θ of Figure 11 is acute.

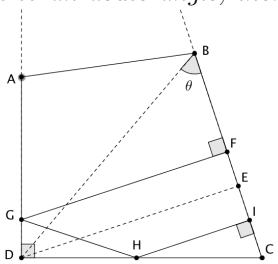

Figure 11

3.4 Opposite acute angles

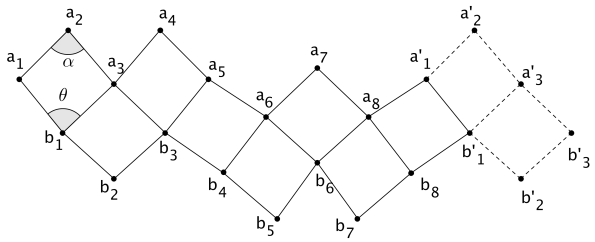

Figure 12: Orbit A

Here we are going to study a specific periodic billiard path with combinatorial orbit 01203213, whose unfolding is illustrated in Figure 12. The last two dotted quadrilateral is a translation of the first two quadrilateral. This orbit is clearly stable by Lemma 2.2.2, and the direction of translation (and thus the direction of the billiard path) is the same as the line connecting b_1 and b_1'. If we let this be the x-axis, and let $y(b_i)$ denote the y-coordinate of b_i (similarly for a_i), then following the discussion after Figure 6, we would like to prove:

Proposition 3.4.1. *If the quadrilateral is $\frac{\pi}{30}$ near square, α, θ in Figure 12 are acute, the other two angles are obtuse, then*

$$\max_j y(b_j) < \min_i y(a_i)$$

and hence the quadrilateral has this periodic path.

Let us start with some observations.

Remark 3.4.2. *If our quadrilateral is $\frac{\pi}{12}$ near square, then* $\max_j y(b_j) = \max\{y(b_1), y(b_3), y(b_6)\}$, *and* $\min_i y(a_i) = \min\{y(a_3), y(a_6), y(a_8)\}$

Proof. Since our quadrilateral is convex, we know $y(a_2)$ is definitely larger than the smaller one of $y(a_1)$ and $y(a_3)$, so we don't need to consider the vertex a_2. Similarly we can eliminate vertices a_4, a_7, b_2, b_5, b_7.

Now suppose that our quadrilateral is $\frac{\pi}{12}$-near square, then we know $\angle b_3a_5a_6 < \frac{2\pi}{3}$, and $\angle a_3a_5b_3 < \frac{\pi}{3}$. So, we know $\angle a_3a_5a_6 < \pi$. So again by convexity, $y(a_5)$ is larger than the smaller one of $y(a_3)$ and $y(a_6)$. In the same fashion, we can eliminate vertices a_1, b_4, b_8. □

So, for Proposition 3.4.1, all that remains is to show:

$$\max\{y(b_1), y(b_3), y(b_6)\} < \min\{y(a_3), y(a_6), y(a_8)\}$$

Note that $y(a_1') = y(a_1), y(b_1') = y(b_1)$. In this section, we use the word 'angular slope' to refer to the angle at which the line meets with the x-axis, i.e. 'angular slope' $= \tan^{-1}(m)$ with values in $\left(-\frac{\pi}{2}, \frac{\pi}{2}\right)$, where m is the gradient of the non-vertical line.

Proposition 3.4.3. *If the quadrilateral is $\frac{\pi}{4}$-near square, then $min(y(a_6), y(a_8)) > max(y(b_1), y(b_3))$ if and only if both α and θ are acute.*

Proof. Let us restrict our attention to $b_1, b_3, a_6, a_8, b_1', b_3'$, as shown in Figure 13a, 13b, 13c, 13d. One can tell from Figure 12 that for the angles *drawn in the Figures below*, $\angle b_1b_3a_6 = \angle a_6a_8b_1' = 2\alpha$, and $\angle b_3a_6a_8 = \angle a_8b_1'b_3' = 2\theta$. Note that $b_1b_3, b_3a_6, a_6a_8, a_8b_1', b_1'b_3'$ all have the same length, since they are the same diagonal of the same quadrilateral. Let us connect b_1a_6 and a_6b_1'. Clearly, $\bigtriangleup b_1a_6b_3 \cong \bigtriangleup b_1'a_6a_8$ are the same isoceles triangle. So, $\angle b_1a_6b_3 = \angle b_1'a_6a_8$, and hence $\bigtriangleup b_1a_6b_1'$ is an isosceles triangle with top angle 2θ or $2\pi - 2\theta$. So if θ is obtuse or right angled, then $y(a_6) \leq 0 = y(b_1)$. Similarly, if α is obtuse or right angled, then observe from $\bigtriangleup b_3a_8b_3'$ that $y(b_3) \geq y(a_8)$.

If both α and θ are acute (see Figure 13d), then $y(a_6) > y(b_1)$ and $y(b_3) < y(a_8)$. Hence, all that remains is to show $y(a_6) > y(b_3)$ and $y(a_8) > y(b_1)$. Using the isosceles triangles $\bigtriangleup b_1a_6b_1'$ and $\bigtriangleup b_1b_3a_6$, we see that the slope of the line b_1b_3 is $\frac{\pi - 2\theta}{2} - \frac{\pi - 2\alpha}{2} = \alpha - \theta$. (Note: if $\alpha < \theta$, then $y(b_3) < y(b_1)$. This following argument is still valid after redrawing Figure 13d accordingly)

One can also see that the slopes of $b_3a_6, a_6a_8, a_8b_1', b_1'b_3'$ are $\pi - \alpha - \theta, \theta - \alpha, \alpha + \theta - \pi, \alpha - \theta$ respectively.

So, to show $y(a_6) > y(b_1)$ and $y(a_8) > y(b_1')$ is equivalent to showing the slope of b_3a_6 is bigger than zero and the slope of a_8b_1' is less than zero (i.e. $0 < \pi - \alpha - \theta < \frac{\pi}{2}$ and $0 > \alpha + \theta - \pi > -\frac{\pi}{2}$). Note that $\alpha, \theta < \frac{\pi}{2}$ implies $\pi - \alpha - \theta > 0$. Furthermore, if the quadrilateral is $\frac{\pi}{4}$-near square, then $\alpha, \theta > \frac{\pi}{4}$, which implies $\pi - \alpha - \theta < \frac{\pi}{2}$. This completes the proof. □

Proposition 3.4.4. *When the quadrilateral is $\frac{\pi}{12}$-near square, then $y(a_3) > \max(y(b_1), y(b_3))$, and $\min(y(a_6), y(a_8)) > y(b_6)$.*

Proof. We know from Proposition 3.4.3 that the slope of b_1b_3 is $\alpha - \theta$, which is between $\frac{\pi}{6}$ and $-\frac{\pi}{6}$ when the quadrilateral is $\frac{\pi}{12}$-near square. As $\angle a_3b_1b_3$ is between $\frac{\pi}{6}$ and $\frac{\pi}{3}$, we see that the slope of b_1a_3 is between $\frac{\pi}{2}$ and 0. So it has positive slope, and $y(a_3) > y(b_1)$. By basically the same argument, we can show that $y(a_3) > y(b_3), y(a_6) > y(b_6), y(a_8) > y(b_6)$. □

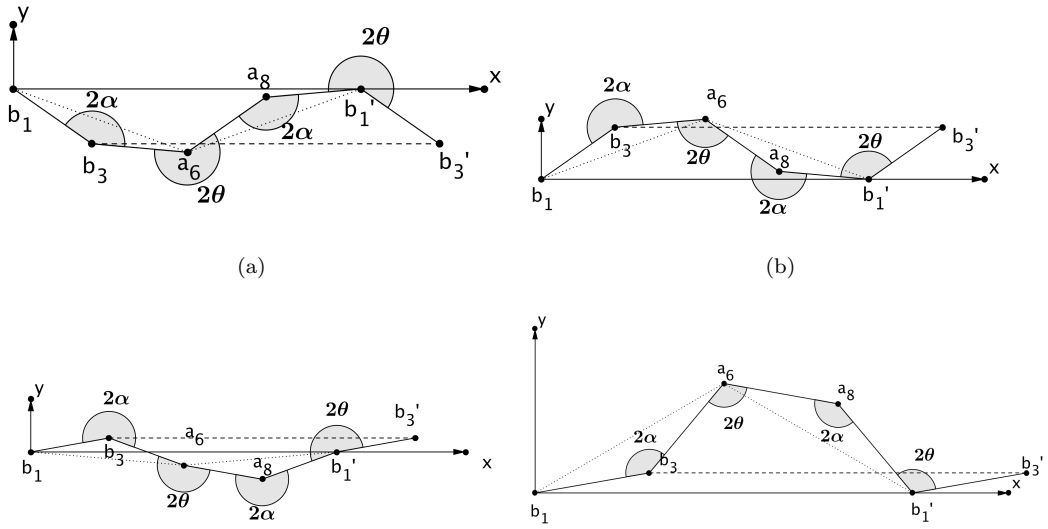

Figure 13: (a)$\alpha < \frac{\pi}{2}$, $\theta > \frac{\pi}{2}$, (b) $\alpha > \frac{\pi}{2}$, $\theta < \frac{\pi}{2}$ (c) $\alpha > \frac{\pi}{2}$, $\theta > \frac{\pi}{2}$ (d) $\alpha < \frac{\pi}{2}$, $\theta < \frac{\pi}{2}$

Lemma 3.4.5. *In an ϵ-near square, if one edge has length 1, then the length of the adjacent edge is between* $\tan\left(\frac{\pi}{4} - \epsilon\right)\cos(2\epsilon)$ *and* $\dfrac{\tan\left(\frac{\pi}{4} + \epsilon\right)}{\cos(2\epsilon)}$.

Proof. WLOG, for Figure 10, let $|AC| = 1$. Then by sine rule:

$$\frac{BC}{AC} = \frac{BC}{1} = \frac{\sin\alpha_1}{\sin\alpha_2}, \qquad \frac{AD}{AC} = \frac{AD}{1} = \frac{\sin\beta_1}{\sin\beta_2} = \frac{\sin\alpha_4}{\sin(\alpha_2+\alpha_4)}\frac{\sin(\alpha_1+\alpha_3)}{\sin\alpha_3}$$

We will leave the rest of the estimation to the reader. □

Proposition 3.4.6. *When the quadrilateral is $\frac{\pi}{30}$-near square, α and θ are acute, and the other two angles are obtuse, then $y(a_3) > y(b_6)$.*

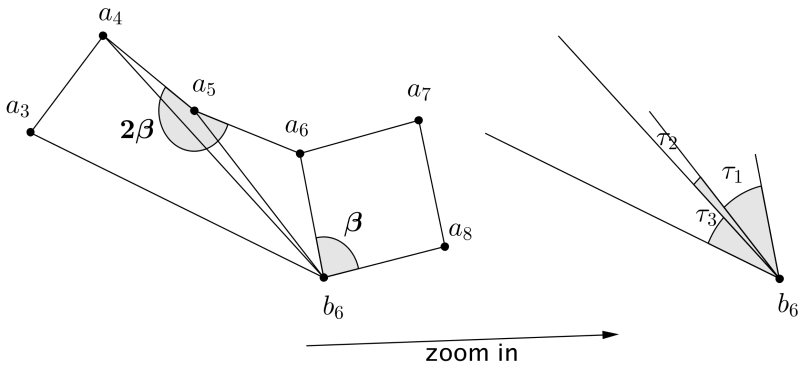

Figure 14

Proof. Clearly the line a_3a_3' is parallel to the x-axis. Then it clearly follows that $y(a_3) > y(b_6)$ if and only if $\angle a_3b_6a_3' < \pi$ (See figure 12)

Let us first look at $\angle a_6b_6a_3$ by breaking it down into three angles, τ_1, τ_2, τ_3, as shown in Figure 14. Suppose our quadrilateral is $\frac{\pi}{30}$-near square, then (See figure 12) $\theta > \frac{\pi}{2} - 2\frac{\pi}{30} = \frac{13\pi}{30}$, so $\angle a_5a_6b_6 = 2\theta > \frac{13\pi}{15}$. As $\bigtriangleup a_5a_6b_6$ is an isosceles triangle, we see that $\tau_1 < \frac{\pi}{15}$. (also, since $\theta < \frac{\pi}{2}$, so $\tau_1 > 0$)

Let $\angle a_6b_6a_8 = \beta$. Then $\angle a_4a_5a_6 = 2\beta$ as shown, and $\angle a_4a_5b_6 = 2\beta - \tau_1 > 2\beta - \frac{\pi}{15}$. If $\angle a_4a_5b_6 \geq \pi$, then $\tau_2 \leq 0$ (i.e. in the figure above, τ_1 and τ_3 overlap). So $\tau_1 + \tau_2 \leq \tau_1 < \frac{\pi}{15}$.

Note that $a_5b_6 = 2\cos(\angle a_6b_6a_5) \cdot a_6b_6 > 2\cos\frac{\pi}{15} * a_6b_6 > a_6b_6 = a_4a_5$. So, if $\angle a_4a_5b_6 < \pi$, then $a_5b_6 > a_4a_5$ implies $\tau_2 < \angle a_5a_4b_6$, hence $\tau_2 < \dfrac{\angle a_5a_4b_6 + \tau_2}{2} = \dfrac{\pi - \angle a_4a_5b_6}{2} < \dfrac{\pi - (2\beta - \frac{\pi}{15})}{2} = \frac{8\pi}{15} - \beta$.

WLOG, let the length $a_4a_5 = a_5a_6 = a_6b_6 = 1$, then we know that $a_5b_6 > 2\cos\frac{\pi}{15}$. Note that $\beta \in (\frac{\pi}{2}, \frac{17}{30}\pi), \tau_1 \in (0, \frac{\pi}{15})$, so $\angle a_4a_5b_6 = 2\beta - \tau_1 \in (\frac{14}{15}\pi, \frac{17}{15}\pi)$ (and hence $\cos(\angle a_4a_5b_6) < 0$).

Then we can see that the length $a_4b_6 > \sqrt{1^2 + (2\cos\frac{\pi}{15})^2 - 2 \cdot 1 \cdot 2\cos\frac{\pi}{15} \cdot \cos(\frac{17}{15}\pi)} \approx 2.89852$. We also know by Lemma 3.4.5 that the length $a_3a_4 < \dfrac{\tan(\frac{\pi}{4} + \frac{\pi}{30})}{\cos\frac{\pi}{15}} \approx 1.26249$. Note that $\sin\tau_3 \leq \dfrac{a_3a_4}{a_4b_6} < \frac{1.26249}{2.89852} \approx 0.43556$. So $\tau_3 < p = 0.45066$.

So now if $2\beta - \frac{\pi}{15} \geq \pi$, then $\angle a_4a_5b_6 \geq \pi$, and so $\tau_1 + \tau_2 + \tau_3 < \frac{\pi}{15} + p$. If $2\beta - \frac{\pi}{15} < \pi$, then $\angle a_6b_6a_3 = \tau_1 + \tau_2 + \tau_3 < (\frac{\pi}{15}) + (\frac{8\pi}{15} - \beta) + p = \frac{3\pi}{5} - \beta + p$. But the latter one is clearly looser in this case, so we use the latter inequality. Similarly, one can also show that $\angle a_3'b_6a_8 < \frac{3\pi}{5} - \beta + p$. So $\angle a_3b_6a_3' < 2(\frac{3\pi}{5} - \beta + p) + \beta < 2p + \frac{6\pi}{5} - \beta < 2p + \frac{6\pi}{5} - \frac{\pi}{2} \approx 3.10043 < \pi$. Here the second to last inequality follows because β is supposed to be obtuse. This proves the proposition.

□

For a summary, a quadrilateral which is $\frac{\pi}{30}$-near square has orbit A if it has two opposite acute angles and two opposite obtuse angles (i.e. it is represented in the region A in Figure 8c).

3.5 The X family orbits

The X family orbits is an infinite family of orbits, starting from X_2. Let us first study X_2, and then study the general pattern of the X family orbits.

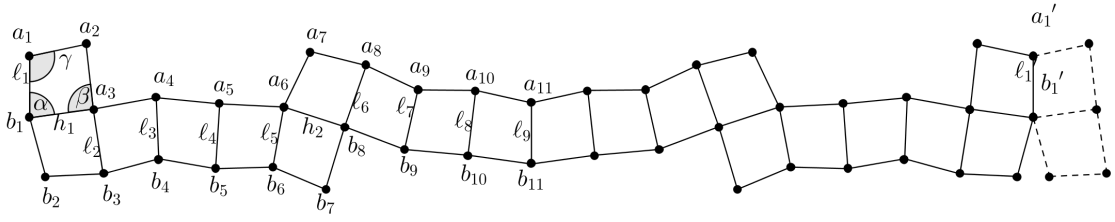

Figure 15: Unfolding of X_2 orbit

Up to a relabeling of the edges, X_2 has the orbit type 01313013131310313103. This is clearly stable by Lemma 2.2.2. An unfolding would look like Figure 15. The first obvious feature of X_2 is that the unfolding is symmetric about the line ℓ_9. Note that the motion from ℓ_1 to ℓ_1' is a translation. So, if

we build a coordinate frame using b_1b_1' as the x-axis and let ℓ_1 as the y-axis, then ℓ_1, ℓ_9, and ℓ_1' are vertical.

Now to find the condition for this orbit to exist, we must find the condition when all top vertices are above all bottom vertices. i.e. in Figure 15, we want to show:

$$\max_j y(b_j) < \min_i y(a_i)$$

Since everything is symmetric about ℓ_9, we only need to consider the left half part of the unfolding. In the following proof, we shall use $v|\ell|w$ to denote the fact that the objects v and w are symmetric about the line ℓ. Furthermore, we shall use $s(\ell)$ to denote the 'angular slope' of the line ℓ ('angular slope' $= \tan^{-1}(m)$ with values in $\left(-\frac{\pi}{2}, \frac{\pi}{2}\right)$, where $m =$ gradient of ℓ). In addition, we use the notation $\min y(a_1, a_2, a_3)$ to denote the minimum of $\{y(a_1), y(a_2), y(a_3)\}$, and similar notation for the maximum.

Proposition 3.5.1. *Suppose the quadrilateral is $\frac{\pi}{16}$-near square, then in Figure 15, TFAE:*

1. $\min y(a_3, a_6) > \max(b_1, b_8)$
2. $s(\ell_3) < 0, s(\ell_4) > 0$ *and* $s(h_1) > 0$.
3. $\alpha < \frac{\pi}{2}, \beta > \frac{\pi}{2}, 3\beta + \alpha < 2\pi$

Proof. (1) $\Rightarrow$ (2): Since $y(a_6) > y(b_1)$ and $b_1|\ell_3|a_6$, we see that $s(\ell_3) < 0$. Since $y(a_3) > y(b_8)$ and $a_3|\ell_4|b_8$, we see that $s(\ell_4) > 0$. Since $y(a_3) > y(b_1)$, we see that $s(h_1) > 0$.

(2) $\Rightarrow$ (3): One can verify that $s(h_1) = \frac{\pi}{2} - \alpha, s(\ell_3) \equiv s(h_1) + 2\beta + \alpha = \frac{\pi}{2} + 2\beta (\text{mod } \pi)$, and $s(\ell_4) \equiv s(\ell_3) + \alpha + \beta = \frac{\pi}{2} + 3\beta + \alpha (\text{mod } \pi)$. Assume for contradiction that $\frac{3\pi}{8} < \beta \leq \frac{\pi}{2}$ (the first inequality is due to the near-squareness). Then $\pi + \frac{1}{4}\pi < 2\beta + \frac{\pi}{2} \leq \pi + \frac{\pi}{2}$. So, after taking modulo π, we get $s(\ell_3) > 0$ (which contradicts (2)). Similarly, we can argue that $\alpha < \frac{\pi}{2}$ and $3\beta + \alpha < 2\pi$.

(3) $\Rightarrow$ (2)&(1): The near square condition also gives us $\alpha > \dfrac{3\pi}{8}, \beta < \dfrac{5\pi}{8}$. So, using the conditions in (3), we can get the inequalities in (2), ℓ_2, h_2 having negative slope and $\ell_5, \ell_6, \ell_7, \ell_8$ having positive slope. Now the slope of h_1, h_2 makes sure that $y(a_3) > y(b_1), y(a_6) > y(b_8)$. And as $b_1|\ell_3|a_6, a_3|\ell_4|b_8$, we have $y(a_6) > y(b_1)$, and $y(a_3) > y(b_8)$. This completes our proof. □

Remark 3.5.2. *If the condition for Prop 3.5.1 is satisfied, and the angle γ is obtuse, then* $\max_j y(b_j) = \max y(b_1, b_4, b_5, b_8), \min_i y(a_i) = \min y(a_3, a_6, a_{11})$

Proof. If γ is obtuse, then immediately we know $y(a_2) > y(a_1), y(a_{10}) > y(a_{11})$, so vertices a_2, a_{10} are eliminated.

Now as $a_3|\ell_3|a_5, a_4|\ell_4|a_6$, by the slope of ℓ_3 and ℓ_4 we must have $y(a_5) > y(a_3), y(a_4) > y(a_6)$. So we don't need to consider vertices a_4, a_5. We also have $b_8|\ell_7|b_{10}, b_9|\ell_8|b_{11}$, so similarly we eliminate vertices b_{10}, b_{11}. We also know that $\angle b_8b_9b_{10} = 2\alpha < 2\pi$, so $y(b_9) < max(y(b_8), y(b_{10}))$, and we eliminate b_9.

As $a_7|\ell_6|a_9, a_8|\ell_7|a_{10}, a_9|\ell_8|a_{11}$, we see that $y(a_7) > y(a_9) > y(a_{11}), y(a_8) > y(a_{10}) > y(a_{11})$, so we eliminate a_7, a_8, a_9. Similarly, as $b_2|\ell_2|b_4, b_3|\ell_3|b_5, b_4|\ell_4|b_6, b_5|\ell_5|b_7$, so $y(b_2) < y(b_4), y(b_3) < y(b_5), y(b_6) < y(b_4), y(b_7) < y(b_5)$. So we eliminate b_2, b_3, b_6, b_7.

Finally, one can use the $\frac{\pi}{12}$ near squareness to estimate and get the result $y(a_1) > y(a_3)$, and so we can eliminate a_1. □

Proposition 3.5.3. *If the condition for Prop 3.5.1 is satisfied, and the quadrilateral is* $\frac{\pi}{56}$*-near square and the angle* γ *is obtuse, then* $\max y(b_1, b_4, b_5, b_8) = \max y(b_1, b_8), \min y(a_3, a_6, a_{11}) = \min y(a_3, a_6)$

Proof. In this proof, we will show that $y(a_{11}) > y(a_6), y(b_4) < y(b_1), y(b_5) < y(b_1)$.

Suppose the length $b_{10}b_{11} = 1$. Then by lemma 3.4.5 we know:

$$y(a_{11}) \geq y(b_{11}) + \tan(\frac{\pi}{4} - \frac{\pi}{56}) \cos\frac{\pi}{28} \approx 0.8880356$$

We can also calculate that:

$$y(a_6) = y(b_{11}) + \cos\alpha - \cos(\alpha + 2\beta) + \cos(3\alpha + 2\beta) - \cos(3\alpha + 4\beta).$$

Note that $\frac{\pi}{2} - 2\varepsilon < \alpha < \frac{\pi}{2}, \beta \geq \frac{\pi}{2}$. So, we have (by letting $\varepsilon = \frac{\pi}{56}$)

$$\begin{aligned} y(a_6) \leq y(b_{11}) &+ \cos\left(\frac{\pi}{2} - 2\varepsilon\right) - \cos\left(\frac{\pi}{2} - 2\varepsilon + 2\cdot\frac{\pi}{2}\right) + \cos\left(3\left(\frac{\pi}{2} - 2\varepsilon\right) + 2\cdot\frac{\pi}{2}\right) \\ &- \cos\left(3\left(\frac{\pi}{2} - 2\varepsilon\right) + 4\cdot\frac{\pi}{2}\right) \approx 0.884487 \end{aligned}$$

A calculation shows that $y(a_{11}) > y(a_6)$.

We have shown that a_{11} is the lowest of a_7, a_8, a_9 and a_{10}. If we draw a line through a_6 perpendicular to ℓ_9, then $a_7, a_8, a_9, a_{10}, a_{11}$ would all lie above this line. So for the same reason, if we draw a line through b_1 perpendicular to ℓ_5, then b_2, b_3, b_4, b_5, b_6 would all lie below this line. As ℓ_5 has positive slope, clearly this perpendicular line has negative slope. So we see that $y(b_4) < y(b_1)$ and $y(b_5) < y(b_1)$. □

By combining the Propositions and Remark, we conclude that a quadrilateral has orbit X_2 if the following conditions are satisfied:

1. the quadrilateral is $\frac{\pi}{56}$-near square;
2. the quadrilateral has one acute angle α, and two obtuse angle adjacent to α;
3. one of the obtuse angle β adjacent to α satisfies the inequalities $2\beta > \pi$ and $\alpha + 3\beta < 2\pi$.

Note that the region X_2 in Figure 8c does satisfy these properties, and hence have this periodic billiard path. (It is also worth mentioning that we do not need β to be the smaller of the two angles adjacent to α.)

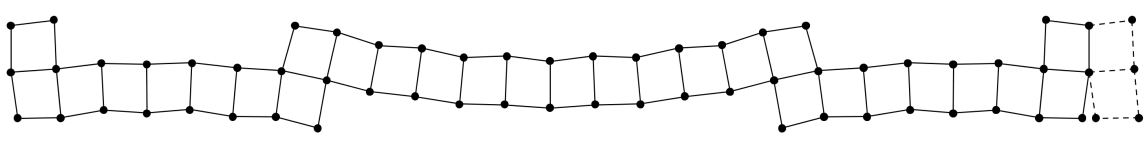

Figure 16: Unfolding of X_3 orbit

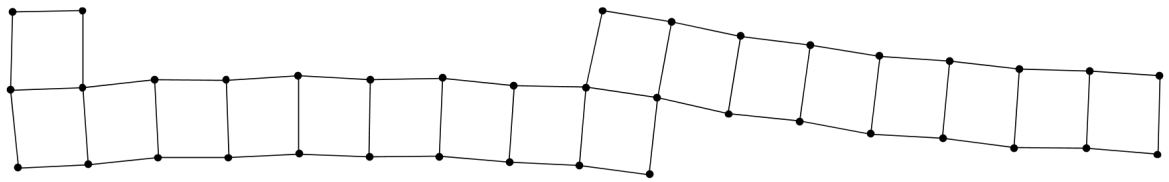

Figure 17: Half unfolding of X_4 orbit

Now we are ready to explore other orbits in the X family. In general, the orbit X_n will have orbit type $0(13)^n0(13)^{n-1}131(31)^{n-1}0(31)^n03$, and some unfolding are in Figure 16, 17. The conditions for these orbits to work is similar to X_2, and the proof is basically identical. For any integer n, a quadrilateral has orbit X_n if the following conditions are satisfied:

1. the quadrilateral is ε_n-near square;
2. the quadrilateral has one acute angle α, and two obtuse angle adjacent to α;
3. one of the obtuse angle β adjacent to α satisfies the inequalities $(n-2)\alpha + n\beta > (n-1)\pi$ and $(n-1)\alpha + (n+1)\beta < n\pi$.

Here ε_n is a decreasing sequence with limit 0 as n goes to ∞. ε_n the real root nearest to 0 of the following equation: Let $x_n = \dfrac{\pi}{2} - 2\epsilon_n, y_n = \dfrac{n-1}{n}\pi - \dfrac{n-2}{n}x_n, y'_n = \frac{\pi}{2}$, then:

$$\tan\left(\frac{\pi}{4} - \varepsilon_n\right)\cos(2\varepsilon_n) = \sum_{i=1}^{n}\cos\left[(2i-1)x_n + (2i-2)y_n\right] - \sum_{i=1}^{n}\cos\left[(2i-1)x_n + (2i)y'_n\right] \qquad (3.5.1)$$

Condition 2 and 3 implies that X_n covers the region T_n in the α-β plane of Figure 18 (as long as the quadrilateral is sufficiently near square). The gradient of L_n is $-\frac{n-1}{n+1}$, which goes to -1 as n goes to ∞. Note that gradient of L_3 is $-1/2$, and the orbit A in Section 3.4 covers the region above the line L_3.

In short, if the quadrilateral is described in region T_3 [T_2, respectively] and is ε_3-near square [ε_2], then it has the orbit X_3 [X_2].

One can calculate that ε_3 is slightly larger than $\frac{\pi}{107}$, and so the near-squareness condition for X_3 is more strict than that of X_2. The only thing left is the lines L_2, L_3, which will be solved by the Y family.

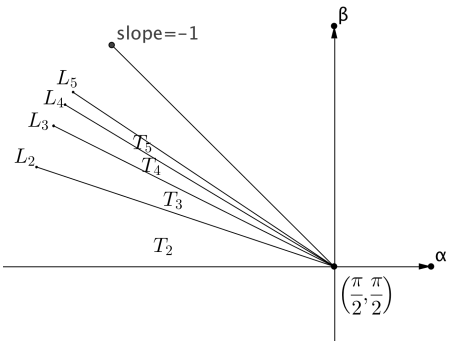

Figure 18: Coordinate Space

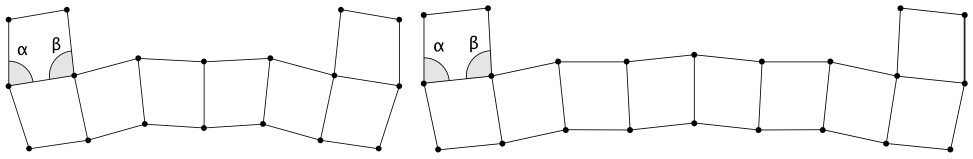

(a) (b)

Figure 19: Unfolding for (a)Y_2, (b) Y_3

3.6 The Y family orbits

The Y family orbits is a family of unstable orbit which covers exactly L_n in Figure 18. Some unfoldings are shown in Figure 19a, 19b with the parameter angle α and β marked.

For example, let us look at X_2 in Figure 15. If the quadrilateral lies on L_2 in the α-β parameter plane, then the line ℓ_4 is vertical. So, if we reflect the first four square in the unfolding of Figure 15, we would get the unfolding in Figure 19a, which we call Y_2. The whole Y family arises this way, and the near-square condition (for this orbit to work) is looser than that for the X family (since there are less vertices to consider compared to X orbits).

To sum up, if a quadrilateral is ε_n-near square and lies on the line L_n in the $\alpha - \beta$ parameter plane, then it has orbit Y_n.

3.7 Summary

So now let us put the whole proof together. Any quadrilateral q, suppose it is $\dfrac{\pi}{107}$-near square.

1. If it is a rectangle, then it has a periodic path where the ball bounces between two parallel lines.
2. If q is not a rectangle, then it has at least one acute angle, call it α. If one of the angle adjacent to α is acute, then q has orbit F. If one of the angle adjacent to α is $90°$, then q has orbit R.
3. Suppose that both angles adjacent to α are obtuse, and let us call the smaller one β, the larger one γ. If the angle opposing α is acute, then q has orbit A.
4. Assume that the angle opposing α is larger than or equal to $\dfrac{\pi}{2}$ and call it θ. Then we know $\alpha + 2\beta + \dfrac{\pi}{2} \leq \alpha + \beta + \gamma + \theta = 2\pi$, so $\alpha + 2\beta \leq \dfrac{3\pi}{2}$. So in the α-β plane, the only region left is T_2, T_3, L_2, L_3. And these regions are covered by orbit X_2, X_3, Y_2, Y_3.

This completes our proof for Theorem 2.2.4.

4 Proof of Theorem 2.2.5

The proof is pretty much identical to that of Theorem 2.2.4. All these orbits still works for rectangles. Fix a rectangle K. For any quadrilateral q, suppose it is sufficiently near K. If q is a rectangle, then clearly it has a periodic path. If it has two adjacent acute angle, then it has orbit F. If it has one

acute angle adjacent to a right angle, then it has orbit R. If it has two acute angle opposing each other, then it will have orbit A.

Suppose it has at least one acute angle α, two adjacent obtuse angle, and the opposite angle to α is not acute. Let β be the smallest of the obtuse angles adjacent to α. Again, we have the inequality $\alpha + 2\beta < \frac{3\pi}{2}$, and the orbits X_2, X_3, Y_2, Y_3 covers these remaining regions in the α-β parameter plane.

The critical question is how near to the fixed rectangle K do we need? Unfortunately this is not easy to answer, as this condition depends on which fixed rectangle K we choose. The "flatter" the rectangle K is, the stricter the condition will need to be.

Acknowledgement. We would like to thank Prof. W Patrick Hooper for his mentoring and support throughout our research, and for providing us with 'McBilliards II', a Java program that searches for periodic billiard paths. We drew lots of observation and inspiration from this Java program. 'McBilliards II' is available online at `http://wphooper.com/visual/mcb2/`.

References

[1] M. Boshernitzan, G. Galperin and T. Krüger and S. Troubetzkoy, Periodic Billiard Orbits Are Dense in Rational Polygons, *Transactions of the American Mathematical Society*, **350(9)** (1998), 3523–3535.

[2] W. P. Hooper and R. E. Schwartz, Billiards in Nearly Isosceles Triangles, *Journal of Modern Dynamics*, **3(2)** (2009), 159–231.

[3] H. Masur and S. Tabachnikov, Rational billiards and flat structures, *Handbook Dynamical Systems*, **1A** (2002), 1015–1089.

[4] R. E. Schwartz, Obtuse Triangular Billiards I: Near the (2,3,6) Triangle, *Journal of Experimental Mathematics*, **15(2)** (2006), 161–182.

[5] R. E. Schwartz, Obtuse Triangular Billiards II: 100 Degrees Worth of Periodic Trajectories, *Journal of Experimental Mathematics*, **18(2)** (2008), 137-171.

[6] S. Tabachnikov, *Billiards*, Panoramas et Synthèses. 1. Paris: Société Mathématique de France. vi, 142 p., 1995.